Is Eurasian snow cover in October a reliable statistical indicator for the wintertime climate on the Iberian Peninsula?

S. Brands[(a)] *, S. Herrera[(b)], J.M. Gutiérrez[(a)]

[(a)]Instituto de Física de Cantabria, CSIC-University of Cantabria, Santander, Spain.

[(b)]Dept. Applied Mathematics and Computer Sciences, University of Cantabria, Santander, Spain.

*Corresponding author address: Swen Brands, Instituto de Física de Cantabria, CSIC-Universidad de Cantabria, Avenida de los Castros s/n, Santander, 39005 Spain.

E-mail: brandssf@unican.es

Abstract

In this study, the recently found lead-lag relationship between Eurasian snow cover increase in October and wintertime precipitation totals on the Iberian Peninsula is revisited and generalized to a broad range of atmospheric variables on the synoptic and local scale. To this aim, a robust (resistant to outliers) method for calculating the index value for Eurasian snow cover increase in October is proposed. This 'Robust Snow Advance Index' (RSAI) is positively correlated with the wintertime (DJF) frequency of cyclonic and westerly-flow circulation types over the Iberian Peninsula, while the corresponding relationship with anticyclonic and easterly-flow types is negative. For both cases, an explained variance of $\sim 60\%$ indicates a strong and highly significant statistical link on the synoptic scale.

Consistent with these findings, it is then shown that the lead-lag relationship equally holds for the DJF-mean conditions of 1) precipitation amount, 2) diurnal temperature range, 3) sun hours, 4) cloud cover, and 5) wind speed on the local scale. To assess if these target variables can be skillfully hindcasted, simple linear regression is applied as a statistical forecasting method, using the October RSAI as the only predictor variable. One-year out cross-validation yields locally significant hindcast correlations of up to ~ 0.8, obtaining field significance for any of the five target variables mentioned above. The validity for a wide range of atmospheric variables and the consistency of the local- and synoptic-scale results affirm the question posed in the title.

KEY WORDS: *Seasonal Forecasting; Teleconnections; Statistical Forecasting; Snow Cover; Climate Variability, Iberian Peninsula*

1. Introduction

Wintertime precipitation totals on the Iberian Peninsula were recently found to be statistically related to Eurasian snow cover increase during the previous October (Brands et al. 2012). A possible dynamical pathway for this formerly unknown lead-lag relationship has been identified by observational and idealized generalized circulation model studies, linking Eurasian snow cover in fall to the Northern Hemisphere extra-tropical circulation during the following winter (Cohen and Entekhabi 1999; Saito et al. 2001; Gong et al. 2003; Cohen et al. 2007; Fletcher et al. 2007, 2009; Smith et al. 2011; Mote and Kutney 2012), the latter commonly described by the Arctic Oscillation (Kutzbach 1970; Thompson and Wallace 1998).

Following the conceptual model in Cohen et al. (2007), a positive snow-cover anomaly in October leads to the early appearance of a strong Siberian cold high, to large amplitudes in the Rossby-wave train and to an upward wave activity flux that weakens the stratospheric polar vortex (Polvani and Waugh 2004). Due to the relatively long de-correlation time of the latter (Baldwin et al. 2003), this weakening/warming persists for several months and propagates downward to the troposphere (Baldwin and Dunkerton 1999), favouring a negative tropospheric AO during the following winter months. Since the North Atlantic Oscillation (NAO) (Walker and Bliss 1932) can be interpreted as a regional manifestation of the AO (Thompson and Wallace 1998), this remote snow forcing is also expected to favour anomalous climate conditions over the North Atlantic and adjacent land areas, such as the Iberian Peninsula (Zorita et al. 1992; Hurrell 1995; Rodriguez-Puebla et al. 2001; Goodess and Jones 2002; Lorenzo et al. 2008).

This study is dedicated to the regional manifestation of this hemispheric-wide teleconnection for the December-to-January (DJF) mean climate on the Iberian Peninsula. To this aim, a robust method for calculating the index value of October Eurasian Snow cover increase (Cohen and Jones 2011) is proposed. This 'Robust Snow Advance Index' is shown to be significantly associated with the DJF circulation characteristics over the Iberian Peninsula, which in turn control the concurrent mean conditions of 1) precipitation amount, 2) diurnal temperature range, 3) sun hours, 4) cloud cover and 5) wind speed on the local/station scale. Finally, it is demonstrated that the latter five variables can be skillfully predicted from Eurasian snow cover increase in October (i.e. with a lead-time of one month) using simple linear regression as a statistical forecasting method.

By linking large-scale predictability to local scale predictability for a wide range of atmospheric variables, this study strengthens the hypothesis that Eurasian snow cover increase is a meaningful statistical predictor for the wintertime-mean climate conditions on the Iberian Peninsula.

2. Data and Methods

Two types of predictand data covering the Iberian Peninsula are used in the present study: 1) large-scale circulation data for calculating weather type frequencies and 2) in-situ station data.

The large scale circulation is represented by daily instantaneous mean sea-level pressure (MSLP) fields at 12 UTC from the ERA-Interim reanalysis (Dee et al. 2011), which were downloaded from ECMWF's public server (`http://data-portal.ecmwf.int/data/d/interim_daily/`). In-situ station data were provided by the European Climate Assessment and Dataset Project (ECA&D, `http://eca.knmi.nl/dailydata/predefinedseries.php`) (Tank et al. 2002; Klok and Tank 2009), documenting daily precipitation amount (in mm), sun hours, cloud cover (in octas), wind speed (daily mean value in m/s) and diurnal temperature range (DTR), the latter obtained by subtracting the daily minimum from the daily maximum temperature and assuming a missing value in case this difference is negative. These station data were downloaded from. A time series is excluded if the percentage of missing values exceeds the 5% threshold. Finally, December-to-February averages are calculated upon the daily values, not taking into account the 29^{th} of February in leap years.

Following Cohen and Jones (2011), snow cover increase over mid-latitudinal Eurasia ($25-60°N$ and $0-180°E$) is calculated for each October between 1997 to 2011 (n = 15), using daily satellite retrievals from the Interactive Multisensor Snow and Ice Mapping System (Ramsay 1998) obtained at `ftp://sidads.`

colorado.edu/pub/DATASETS/NOAA/G02156/24km/. For a given October, the snow cover extension over the above mentioned spatial domain is calculated for each of the 31 days, yielding a sample of 31 square kilometer values. The index value describing snow cover advance is then defined as the regression coefficient (i.e. the slope) of the linear regression line fitted to this sample. A visual inspection of the daily snow cover time series revealed the presence of large and rapid snow cover increases, which are especially prominent in October 2011 (see last two days in Fig. 1b). Since this snow cover 'surges' are outliers from a statistical point of view, and since ordinary least-squares regression is known to be sensitive to outliers, a robust linear regression method for calculating snow cover increase is proposed as an improvement of the original definition of the 'Snow Advance Index' (SAI) (Cohen and Jones 2011). This method gives less weight to outlier data points when fitting the regression line and essentially removes outlier-related uncertainty (Street et al. 1988). The slope/regression coefficient obtained from robust linear regression is then defined as the 'Robust Snow Advance Index' (RSAI) and the 15 index values for October 1997 to 2011 are standardized to have zero mean and unit variance. As shown in Fig. 1 for the case of October 2011 (panel b) as compared to October 2009 (panel a), the modified index differs considerably from the original one if outliers are present in the underlying data. Fig. 1c shows the comparison between both indices for the fifteen October months between 1997 (when satellite-sensed snow cover data on daily timescale became available) and 2011, exhibiting large differences for October 2011. For a detailed description of the applied robust linear regression method, the reader is referred to the appendix of the present study.

To compute discrete weather types from continuous daily MSLP patterns, the automated Lamb weather typing (LWT) approach is applied (Jenkinson and Collison 1977; Jones et al. 1993). The LWT-specifications described in Trigo and DaCamara (2000) have been adopted, using daily MSLP data at 12 UTC from ERA-Interim covering all DJF-days between 1997/98 and 2011/12. The reanalysis data are linearly interpolated to the 16 grid-boxes shown in Fig. 2a), forming a 'cross' centered over the Iberian Peninsula. Following Trigo and DaCamara (2000), we opt for classifying all days, i.e. work with 26 classes instead of the original 27 classes. Composite maps showing the temporal mean of the MSLP values corresponding to a given weather type (i.e. the conditional mean) have been calculated to assure that the LWTs are physically meaningful. These composite maps are similar to those obtained in Trigo and DaCamara (2000) and the 14 WTs considered in this study are displayed in Fig. 2.

In contrast to other automated classification techniques like 'Self Organizing Maps' (Hewitson and Crane 2002; Gutierrez et al. 2005) or 'k-means clustering' (Gutierrez et al. 2004), LWT is a rule-based classification scheme where the classes are pre-defined based on meteorological expert knowledge (Lamb 1972). This is convenient for the present type of study, since applying stochastic classification schemes would lead to slight differences in the obtained frequencies of weather types, caused by the fact that some days would be assigned to different classes in different realizations. This, in turn, would inhibit a proper estimate of statistical significance when correlating weather type frequencies against another variable (Hewitson and Crane 2002), that is the RSAI in the present study.

To reveal the statistical relationship between the RSAI and the target variables on the Iberian Peninsula, the Pearson correlation coefficient (hereafter 'Pearson correlation' or 'r') is used. Due to the short sample size ($n = 15$), which is imposed by the availability of daily snow cover data (Ramsay 1998), outlier-presence can falsify the results of the correlation analysis. For instance, the DJF-season 2009/10 was characterized by an extremely negative phase of the AO and NAO (Cohen et al. 2010), associated with largely anomalous values for the concurrent climate conditions on the Iberian Peninsula (Vicente-Serrano et al. 2011). To check the robustness of the results to this 'outlier-winter', the non-parametric Spearman rank correlation coefficient (hereafter 'Spearman correlation' or 'rs') is used in addition (Wilks 2006).

To test if the DJF-mean target variables can be hindcasted from the October RSAI, simple linear regression is applied in a one-year-out cross-validation framework (Michaelsen 1987), using the RSAI as the only predictor variable. Note that the predictor-predictand pairs withheld in each step of the cross-validation are not truly independent since all predictor-predictand pairs (i.e. the whole available time series) have been used for searching the statistical relationship between October Eurasian snow cover and the DJF-mean climate on the Iberian Peninsula (DelSole and Shukla 2009). Consequently, our results obtained from cross-validation (see Sec. 4) might suffer from artificial skill, i.e. might not reflect the skill the statistical 'forecasting' method would obtain in real/future forecast situations (see also Sec. 5). Therefore, when referring to statistical 'predictions' obtained from cross-validation, we will use the term 'hindcast' instead of 'forecasts'.

Note also that using robust- instead of ordinary regression as a statistical forecasting method leads to virtually identical results. Therefore, the results obtained from the simpler method (i.e. ordinary regression) will be shown in Sec. 4. To exclude the possibility that the results of the one-year-out cross-validation could be biased by linear trends, the predictor / predictand samples used to obtain the forecast equation (sample size: $n-1$) are linearly de-trended and centered to have zero mean. To eliminate a further potential source of dependency / artificial skill, the trend and mean removal is repeated in each step of the cross-validation (von Storch and Zwiers 1999), i.e. the i^{th} forecast is obtained from predictor / predictand samples having no linear trend and zero mean in any case. Note that the trends and means obtained in the i^{th} step of the cross-validation are also removed from the i^{th} withheld predictor and predictand values respectively.

To assess the skill obtained from cross-validation, the hindcasted time series are compared to their observed counterparts by using the Pearson correlation coefficient. The corresponding results will be referred to as 'hindcast correlations' (Folland et al. 2012) in the forthcoming. Local statistical significance is assessed with a two-sided t-test (H_0 = zero correlation) and global significance is tested by repeating the cross-validation procedure 2000 times. In each repetition, the RSAI time series is randomly re-ordered following the ranks of a random sample of integers drawn from the standard uniform distribution. Then, the percentage of significant local hindcast skill ($\alpha_{local} = 0.05$) obtained by chance is calculated and saved. The 99^{th} percentile of the resulting sample of 2000 percentage values is the critical value above which global significance (α_{global}) is assumed at a test-level of 1%.

Apart from forecasting with the October RSAI, the one-year-out cross-validation approach is additionally applied for the October SAI, i.e. for the original Snow Advance Index described in Cohen and Jones (2011), as well as for the October monthly-mean NAO and AO indices (both based on Principal Component Analysis) as defined by Hurrell et al. (2003) (http://climatedataguide.ucar.edu/es/guidance/hurrell-north-atlantic-oscillation-nao-index-pc-based) and the Climate Prediction Center (www.cpc.ncep.noaa.gov/products/precip/CWlink/daily_ao_index/ao_index.html) respectively.

In addition to the Pearson correlation, the root mean squared error skill score (rmsess) is applied for assessing the out-of-sample skill (Jolliffe and Stephenson 2003):

$$rmsess = (1 - \frac{rmse}{rmse_{ref}}) \times 100 \qquad (1)$$

where $rmse$ is the root-mean squared error of the time series predicted by the statistical forecasting method described above and $rmse_{ref}$ is the $rmse$ obtained from always predicting the climatological mean, which is zero in any case since anomalies are forecasted. Thus, $rmsess$ gives the percentage with which the purely climatological forecast is outperformed by predicting from October Eurasian snow cover increase.

3. Relevance of serial correlation

There are two potential reasons why positive serial correlation could adversely affect the results of the present study. First, and if not accounted for (see Eq. 2), positive serial correlation leads to too-many type one errors due to an artificial lowering of the correlation coefficient's $p - value$, arising from the fact that the number of temporally independent data pairs is lower than the sample size (Trenberth 1984; Kristjansson et al. 2002). Therefore, the $p - value$ is calculated upon the *effective sample size* (n^*):

$$n^* = n\frac{1 - l_1 l_2}{1 + l_1 l_2} \qquad (2)$$

where n is the sample size and l_1 (l_2) is the lag-1 autocorrelation coefficient of time series 1 (2) (Bretherton et al. 1999; Beranova and Huth 2007). Note that the time series are assumed to follow a first-order autoregressive process and that the effective number of degrees of freedom for the two-sided t-test is $n^* - 2$.

Second, positive serial correlation questions the applicability of the one-year-out cross-validation approach which assumes zero serial correlation for the predictor/predictand time series (Michaelsen 1987). To assess the degree to which our forecast skill estimates are affected by serial correlation, Fig. 2 displays the spatial distribution of the lag-1 autocorrelation coefficients ($r - lag1$) obtained from the 61-66 samples of each predictand variable (note that the number of station time series slightly varies from one variable to another). As can be seen from the figure, the median (bar of the boxplot) ranges between ± 0.1 and the interquartile range (box of the boxplot) between ± 0.2 for any of the applied variables, i.e. the samples are approximately centered around zero. Due to the limited sample size, critical values for significantly positive $r - lag1$ (note that the t-test should be one-sided since only positive values of $r - lag1$ decrease the effective sample size) would be high even for a local test level of 10%. Therefore, $r - lag1 > +0.25$ was defined as an alternative threshold above which serial correlation would have a measurable effect on cross-validation estimates of forecast skill, as was originally proposed by Michaelsen (1987). The percentage of time series exceeding this threshold (which will hereafter referred to as 'problematic') can be obtained from Tab. 1 for each predictand variable under study. For all predictand variables except wind speed, less than 5% of the applied time series suffer from a problematic serial correlation.

To additionally assess if the areal fraction of problematic serial correlations is *globally* significant, the following Monte-Carlo technique is applied separately for each of the 5 predictand variables. First, the temporal sequence of all time series corresponding to a given predictand variable is randomly re-ordered following the the ranks of a random sample of integers drawn from the standard uniform distribution. Since this re-ordering is identical for all time series of a given predictand variable, the spatial autocorrelation of the field is maintained whereas the serial correlation is eliminated. Then, the areal fraction for which $r - lag1 > +0.25$ by chance is calculated and saved. After repeating the whole procedure 2000 times, the 90^{th} (95^{th}) percentile of the resulting 2000 areal fractions for which $r - lag1 > +0.25$ by chance is assumed as the critical value above which the fraction of local $r - lag1 > 0.25$ obtained from the correct time series (i.e. having the correct temporal order) is globally significant at a test-level of 10% (5%). Even for a global test-level of 10% ($\alpha_{global} = 0.10$), in which case the global H_0 ('the observed fraction of $r - lag1 > +0.25$ arises from chance') is easier to reject than for assuming $\alpha_{global} = 0.05$, the H_0 cannot be rejected for any single predictand variable (see Tab. 1).

On the basis of these results, we conclude that the hindcast skill estimates obtained from one-year-out cross-validation (see Sec. 4) are generally not seriously affected by serial correlation.

4. Results

Figure 5 shows the composite maps of the 14 weather types relevant for the present study. For the ease of understanding, the panels of the figure are ordered to follow the cardinal directions, i.e. westerly flow types are displayed on the left hand side and easterly ones are shown on the right hand side. 'CNW' is the acronym for 'cyclonic northwest', 'ANE' for 'anticyclonic northeast', etc. Above each panel, two numbers are displayed. The first refers to the number of the weather type and the second to its relative frequency (in %) over the whole period under study (DJF 1997/98 to 2011/12). For an adequate visualization of the direction of the geostrophic flow (hereafter: 'flow'), 10 isobars are displayed in each panel. The pressure gradient can be derived from the color shading.

With a relative frequency of 55.8%, the wintertime circulation over the Iberian Peninsula is dominated by anticyclonic and easterly flow conditions, while cyclonic and westerly flow conditions occur on 22.5% of the days. The spatial patterns of the rare hybrid weather types (4, 5, 6 and 9, 10, 11) are similar to their more frequently occurring purely directional flow counterparts (1, 2 ,3 and 12, 13, 14). In order to obtain an adequate sample size for each of the 15 winter seasons, and similar to the approach applied in Trigo and DaCamara (2000), the DJF-frequencies/counts of the cyclonic and westerly flow types on the one hand and those of the anticyclonic and easterly flow types on the other are aggregated to two groups with opposite vorticity and flow characteristics. The corresponding two composite maps are shown in Fig. 5a) and b). With a standard deviation of 12 and 14 days from a mean of 20 and 50 days respectively, the yearly DJF-counts of both groups are characterized by a large inter-annual variability, especially in case of the cyclonic and westerly flow group.

The second row of Fig. 5 indicates that this inter-annual variability is statistically related to Eurasian snow cover increase in October as represented by the RSAI, yielding a fraction of explained variance of approximately 60% for both of the above mentioned groups. With a Pearson / Spearman correlation of +0.76 / +0.83, this relationship is positive for the frequency of cyclonic and westerly flow types (see Fig. 5c) while an inverse relationship of -0.80 / -0.86 is found for the anticyclonic and easterly flow types (see Fig. 5d). Note that the linear trend of the frequency time series has been removed before computing these correlations and that the anomalies of the de-trended time series are displayed in Fig.5c+d. The RSAI is displayed in standardized anomalies. Since both the Pearson and Spearman correlations are significant at a test level of 1%, and since the results for the non-detrended time series (see parentheses in Fig.5c+d) are similar, the strong statistical relationships are 1) very unlikely to be a product of chance, 2) insensitive to outlier values and 3) insensitive to possible trends in the underlying data.

To link synoptic and local scale predictability, Figure 5 shows the mean values, conditioned to the two defined groups, for precipitation amount, DTR, sun hours, cloud cover and wind speed at the available weather stations. In the left column, the mean of the local values pertaining to cyclonic and westerly flow days is displayed at each site, while in the right column the corresponding results for the anticyclonic and easterly flow days are shown. The mean surface climate associated to cyclonic and westerly flow types is generally characterized by wetter conditions, a reduced DTR, less sun hours, cloudier skies and windier conditions than it is the case for the anticyclonic and easterly flow types.

Since it has been shown that Eurasian snow cover increase is a significant predictor of the DJF-circulation dynamics over the Iberian Peninsula, which in turn control the concurrent mean conditions of various climate variables on the local scale, the latter will be directly hindcasted from the October RSAI in the next step of the study. Fig. 6 shows the hindcast correlations obtained from one-year-out cross-validation (see Section 2), which are only shown in case they are significant at a test-level of 5% (the critical value is not constant since it depends on the effective sample size n^* defined in Eq. 2). Note that spurious hindcast correlations are marked by a black cross and that the mean and maximum of the significant values is shown in the upper left corner of each panel. With hindcast correlations of up to 0.92, 0.89, 0.88, 0.80 and 0.79 for precipitation amount, DTR, sun hours, cloud cover and wind speed respectively (see left column of Fig.6), the skill of the proposed statistical forecasting method is significant over a large fraction of the study area, this fraction being smallest for the case of wind speed. The climatological (no-skill) hindcast is outperformed by up to 60, 55, 52, 39 and 37% for the five above mentioned variables (see right column of Fig.6), demonstrating that the skill is robust to applying an alternative measure. Note that these results are obtained from detrending the predictor and predictand samples in each step of the cross validation. Using the original / non-detrended timeseries (not shown) yields similar skill levels, indicating that the results are not sensitive to possible trends in the underlying data. Note also that the Pearson correlation between the RSAI and the target variables, i.e. the within sample relationships (not shown) are systematically stronger than the hindcast correlations obtained from cross-validation. The sign of the correlation between the RSAI and the target variables is spatially homogeneous and is shown in the lower left corner of each panel.

Using the RSAI instead of the outlier sensitive SAI (Cohen and Jones 2011) systematically enhances the hindcast skill obtained from cross-validation for all applied variables. Tab. 2 documents this by comparing the areal fraction of locally significant ($\alpha_{local} = 0.05$) hindcast correlations obtained from the RSAI to the respective areal fraction obtained from the SAI (see columns 2+3). For any of the 5 target variables, the 99^{th} percentile of the 2000 fractions obtained from the randomly re-shuffled RSAI is much lower than the fraction obtained from the 'correct' RSAI (i.e. having the correct temporal order). Hence, field significance ($\alpha_{local} = 0.05$, $\alpha_{global} = 0.01$) is given in any case. Moreover, the areal fractions obtained from using the October-mean NAO (or AO) index as single predictor instead of the RSAI are comparatively low (see columns 4+5). This indicates that the hindcast skill stemming from the NAO (or AO) anomaly in October, which potentially could persist throughout the following winter months, is negligible.

5. Discussion and Conclusions

This study has provided further statistical evidence for the existence of a formerly unknown lead-lag relationship between Eurasian snow cover increase in October and the winter climate on the Iberian Peninsula (Brands et al. 2012). It has been found that an anomalously high increase of Eurasian snow cover in October favours an above normal frequency of cyclonic and westerly flow weather situations over the Iberian Peninsula during the following December-to-February season, whereas the frequency of anticyclonic and easterly flow situations is below normal. With an explained variance of $\sim 60\%$ for both groups of circulation types, this statistical relationship is strong and highly significant ($\alpha = 0.01$). At the local-scale, this favors below-normal DJF-mean conditions for diurnal temperature range and sun hours, while the corresponding values for cloud cover, wind speed and precipitation amount are above-normal.

On the basis of these results, it has been additionally shown that the above mentioned variables can be skillfully hindcasted using simple linear regression in a one-year-out cross-validation framework. Locally significant hindcast correlations of up to 0.92, 0.89, 0.88, 0.80 and 0.79 where found for precipitation amount, diurnal temperature range, sun hours, cloud cover and wind speed respectively, the corresponding skill patterns being globally significant in any case ($\alpha_{local} = 0.05$, $\alpha_{global} = 0.01$). Applying robust linear regression instead of ordinary linear regression (Cohen and Jones 2011) for calculating October snow cover increase was found to improve the statistical relationship. Due to the limited sample size, we cannot judge the significance of this improvement yet.

The conducted tests for local and global significance and the consistency of the results for a broad range of atmospheric variables on the local and synoptic scale indicate that the described teleconnection is very unlikely to be by chance and that the question posed in the title can be affirmed. However, the limited size of the samples available to-date ($n = 15$) poses some restrictions on this conclusion. First, it was not possible to test the validity of the teleconnection / skill of the statistical forecasting scheme for a large independent time period. Actually, the strength of the statistical link between large-scale circulation indices (such as the

NAO or AO) and the surface climate on the Iberian Peninsula is known to be non-stationary (Rodo et al. 1997; Beranova and Huth 2007) and a similar behaviour would be expected for the teleconnection suggested here. In this context, it is also important to note that the data withheld in each step of the one-year-out cross-validation is not a surrogate of truly independent/future data since, prior to cross-validation, all data pairs had been used for detecting the teleconnection, as is commonly done in this type of studies [see DelSole and Shukla (2009) and references therein]. Consequently, the proposed teleconnection should be re-tested in the future, when a larger samples of independent predictor-predictand pairs become available (Labitzke et al. 2006). Finally, it is recommended to assess the atmospheric precursors of October Eurasian snow cover increase in order to challenge the causal relationship suggested in the present study.

Our results are expected to be of value for the purpose of statistical seasonal prediction and its applications (Brands 2013). One evident message is to include the Robust Snow Advance Index as an additional informative predictor of multiple linear or nonlinear predictions schemes (Tangang et al. 1997; Rodriguez-Fonseca and de Castro 2002; Hertig and Jacobeit 2011; Lorenzo et al. 2011; Folland et al. 2012). Our results are also expected to be of interest for the numerical climate modeling community. First, general circulation models (GCMs) run in seasonal prediction mode are known to have little skill in predicting the boreal winter climate (Doblas-Reyes et al. 2009; Frias et al. 2010; Kim et al. 2012). Second, transient GCM simulations run over climatic periods of the historical past (Taylor et al. 2012) are known to overestimate the boreal winter westerlies over the North Atlantic (Brands et al. 2013; Zappa et al. 2013). These GCM-errors might be attributed to poor snow-atmosphere / troposphere-stratosphere coupling and improvements in these fields may consequently help to improve the models (Hardiman et al. 2008; Charlton-Perez et al. 2013).

On the other hand, the purely statistical relationships described in the present study are incomplete without assessing the physical background of the teleconnection with idealized numerical model studies. In this context, it is important to note that some of the idealized numerical model studies conducted to-date do not support the strong two-way troposphere-stratosphere coupling described above (see Sec. 1), but suggest a purely tropospheric pathway (Peings et al. 2012; Orsolini et al. 2013). A further argument against a circulation pathway involving a strong two-way troposphere-stratosphere coupling (Cohen et al. 2007) are the findings of Baldwin et al. (2003) who state that only $\sim 20\%$ of the variance of the boreal winter AO can be explained by downward propagation from the stratosphere. This is in disagreement with the much larger fraction of variance of winter climate anomalies on the Iberian Peninsula that can be explained by October Eurasian snow cover increase (e.g. $\sim 60\%$ for the case of weather type frequencies). To put it in another way, if *one-way* downward propagation accounts for only $\sim 20\%$ of the variance of the *hemispheric-wide* circulation in boreal winter (as described by the AO), how is it possible that *two-way* troposphere-stratosphere coupling accounts for a much larger fraction of variance of the *regional* winter climate on the Iberian Peninsula? Consequently, both statistical and numerical modelers can learn from each other while further investigating the lead-lag relationships between Eurasian snow cover in fall and the boreal winter climate.

Acknowledgement This study was funded by the EU project SPECS funded by the European Commissions Seventh Framework Research Programme under the grant agreement 243964. S.B. would like to thank the 'Consejo Superior de Investigaciones Científicas' for financial support. The authors acknowledge the ERA-Interim (http://www.ecmwf.int/research/era/do/get/era-interim), ECA&D (http://eca.knmi.nl/) and E-OBS (`http://ensembles-eu.metoffice.com/`) datasets. They are grateful to Dr. Colin Harpham (Climate Research Unit) for providing programming details on the automated Lamb weather typing approach and would like to thank Dr. Nieves Lorenzo (University of Vigo), acting as a reviewer, and one anonymous reviewer for their helpful comments on the former version of this manuscript. Finally, the authors would like to thank Dr. Michael Riemer (University of Mainz) for a critical comment on the interpretation of our results.

Appendix

Consider the regression equation:

$$y_i = \beta x_i + \sigma e_i, \tag{3}$$

where y_i is the daily snow cover extension for the day x_i, β is the regression coefficient, σ is the error scale parameter and e_i is the error assumed to be independent and identically distributed. Then, iteratively re-weighted least-squares regression is used as follows (Street et al. 1988):

1. Obtain an initial estimate $\bar{\beta}$ for β, as well as the residuals r_i by performing a least squares regression on $y_i = \beta x_i$
2. Obtain an estimate $\bar{\sigma}$ for σ, where $\bar{\sigma} = MAD_r/0.6745$, and MAD_r is the median absolute deviation of the residuals from their median.
3. Re-calculate the residuals $r_i = (y_i - x_i\bar{\beta})/\bar{\sigma}$
4. For any $R_i < \pi$, a weighting term $w_i = sin(r_i)/R_i$ is defined, where $R_i = r_i/(1.339*(MAD_r/0.6745)*\sqrt{(1-h)})$ and h is the leverage obtained from a least-squares fit. Note that this weighting function was published by Andrews (1974) and that alternative functions (Huber 2009) yielded virtually identical results.
5. Update the estimate $\bar{\beta}$ as well as the residuals r_i by performing a least squares regression with the weights w_i.
6. Repeat steps (2) to (5) until MAD_r is minimized.

The 'Robust Snow Advance Index' (RSAI) is then defined as the regression coefficient β obtained from this iterative optimization procedure, performed with the *robustfit.m* function of the programming environment *Matlab*®. Finally, the 15 RSAI index values obtained for each October are z-transformed to yield standardized anomalies.

References

Andrews, D., 1974: A Robust method for multiple linear-regression. *Technometrics*, **16 (4)**, 523–531, doi: {10.2307/1267603}.

Baldwin, M. P. and T. J. Dunkerton, 1999: Propagation of the Arctic Oscillation from the stratosphere to the troposphere. *Journal of Geophysical Research - Atmospheres*, **104 (D24)**, 30 937–30 946, doi: {10.1029/1999JD900445}.

Baldwin, M. P., D. B. Stephenson, D. W. J. Thompson, T. J. Dunkerton, A. J. Charlton, and A. O'Neill, 2003: Stratospheric memory and skill of extended-range weather forecasts. *Science*, **301 (5633)**, 636–640, doi:{10.1126/science.1087143}.

Beranova, R. and R. Huth, 2007: Time variations of the relationships between the north atlantic oscillation and european winter temperature and precipitation. *Studia Geohphysica et Geodaetica*, **51 (4)**, 575–590, doi:{10.1007/s11200-007-0034-3}.

Brands, S., 2013: Skillful seasonal predictions of boreal winter accumulated heating degree days and relevance for the weather derivative market. *Journal of Applied Meteorology and Climatology*, doi: 10.1175/JAMC-D-12-0303.1.

Brands, S., S. Herrera, J. Fernandez, and J. Gutierrez, 2013: How well do CMIP5 Earth System Models simulate present climate conditions in Europe and Africa? A performance comparison for the downscaling community. doi:10.1007/s00382-013-1742-8.

Brands, S., R. Manzanas, J. M. Gutierrez, and J. Cohen, 2012: Seasonal Predictability of Wintertime Precipitation in Europe Using the Snow Advance Index. *Journal of Climate*, **25 (12)**, 4023–4028, doi: {10.1175/JCLI-D-12-00083.1}.

Bretherton, C., M. Widmann, V. Dymnikov, J. Wallace, and I. Blade, 1999: The effective number of spatial degrees of freedom of a time-varying field. *Journal of Climate*, **12 (7)**, 1990–2009, doi:{10.1175/1520-0442(1999)012⟨1990:TENOSD⟩2.0.CO;2}.

Charlton-Perez, A., et al., 2013: On the lack of stratospheric dynamical variability in low-top versions of the CMIP5 models. **118 (6)**, 2494–2505, doi:DOI:10.1002/jgrd.50125.

Cohen, J., M. Barlow, P. J. Kushner, and K. Saito, 2007: Stratosphere-troposphere coupling and links with Eurasian land surface variability. *Journal of Climate*, **20 (21)**, 5335–5343, doi:{10.1175/2007JCLI1725.1}.

Cohen, J. and D. Entekhabi, 1999: Eurasian snow cover variability and Northern Hemisphere climate predictability. *Geophysical Research Letters*, **26 (3)**, 345–348, doi:{10.1029/1998GL900321}.

Cohen, J., J. Foster, M. Barlow, K. Saito, and J. Jones, 2010: Winter 2009-2010: A case study of an extreme Arctic Oscillation event. *Geophysical Research Letters*, **37**, doi:{10.1029/2010GL044256}.

Cohen, J. and J. Jones, 2011: A new index for more accurate winter predictions. *Geophysical Research Letters*, **38**, doi:{10.1029/2011GL049626}.

Dee, D. P., et al., 2011: The ERA-Interim reanalysis: configuration and performance of the data assimilation system. *Quarterly Journal of the Royal Meteorological Society*, **137 (656, Part a)**, 553–597, doi:{10.1002/qj.828}.

DelSole, T. and J. Shukla, 2009: Artificial Skill due to Predictor Screening. *Journal of Climate*, **22 (2)**, 331–345, doi:{10.1175/2008JCLI2414.1}.

Doblas-Reyes, F. J., et al., 2009: Addressing model uncertainty in seasonal and annual dynamical ensemble forecasts. *Quarterly Journal of the Royal Meteorological Society*, **135 (643)**, 1538–1559, doi:{10.1002/qj.464}.

Fletcher, C. G., S. C. Hardiman, P. J. Kushner, and J. Cohen, 2009: The dynamical response to snow cover perturbations in a large ensemble of atmospheric GCM integrations. *Journal of Climate*, **22 (5)**, 1208–1222, doi:{10.1175/2008JCLI2505.1}.

Fletcher, C. G., P. J. Kushner, and J. Cohen, 2007: Stratospheric control of the extratropical circulation response to surface forcing. *Geophysical Research Letters*, **34 (21)**, doi:{10.1029/2007GL031626}.

Folland, C. K., A. A. Scaife, J. Lindesay, and D. B. Stephenson, 2012: How potentially predictable is northern European winter climate a season ahead? *International Journal of Climatology*, **32 (6)**, 801–818, doi:{10.1002/joc.2314}.

Frias, M. D., S. Herrera, A. S. Cofino, and J. M. Gutierrez, 2010: Assessing the skill of precipitation and temperature seasonal forecasts in Spain: windows of opportunity related to ENSO events. *Journal of Climate*, **23 (2)**, 209–220, doi:{10.1175/2009JCLI2824.1}.

Gong, G., D. Entekhabi, and J. Cohen, 2003: Modeled Northern Hemisphere winter climate response to realistic Siberian snow anomalies. *Journal of Climate*, **16 (23)**, 3917–3931, doi:{10.1175/1520-0442(2003)016⟨3917:MNHWCR⟩2.0.CO;2}.

Goodess, C. M. and P. D. Jones, 2002: Links between circulation and changes in the characteristics of Iberian rainfall. *International Journal of Climatology*, **22 (13)**, 1593–1615, doi:{10.1002/joc.810}.

Gutierrez, J., A. Cofino, R. Cano, and M. Rodriguez, 2004: Clustering methods for statistical downscaling in short-range weather forecasts. *Monthly Weather Review*, **132 (9)**, 2169–2183, doi:{10.1175/1520-0493(2004)132⟨2169:CMFSDI⟩2.0.CO;2}.

Gutierrez, J. M., R. Cano, A. S. Cofino, and C. Sordo, 2005: Analysis and downscaling multi-model seasonal forecasts in Peru using self-organizing maps. *Tellus A*, **57 (3)**, 435–447, doi:{10.1111/j.1600-0870.2005.00128.x}.

Hardiman, S. C., P. J. Kushner, and J. Cohen, 2008: Investigating the ability of general circulation models to capture the effects of Eurasian snow cover on winter climate. *Journal of Geophysical Research - Atmospheres*, **113 (D21)**, doi:{10.1029/2008JD010623}.

Hertig, E. and J. Jacobeit, 2011: Predictability of Mediterranean climate variables from oceanic variability. Part II: Statistical models for monthly precipitation and temperature in the Mediterranean area. *Climate Dynamics*, **36 (5-6)**, 825–843, doi:{10.1007/s00382-010-0821-3}.

Hewitson, B. and R. Crane, 2002: Self-organizing maps: applications to synoptic climatology. *Climate Research*, **22 (1)**, 13–26, doi:{10.3354/cr022013}.

Huber, P., 2009: *Robust statistics*. 2 ed., Wiley, Hoboken - New Jersey.

Hurrell, J., Y. Kushnir, G. Ottersen, and M. Visbeck, 2003: *The North Atlantic Oscillation: Climate Significance and Environmental Impact*, Geophysical Monograph Series, Vol. 134. AGU, Washington, D. C., 279 pp.

Hurrell, J. W., 1995: Decadal trends in the North-Atlantic Oscillation - regional temperatures and precipitation. *Science*, **269 (5224)**, 676–679, doi:{10.1126/science.269.5224.676}.

Jenkinson, A. and F. Collison, 1977: *An initial climatology of gales over the North Sea*, Synoptic Climatology Branch Memorandum, Vol. 62. Meteorlogical Office, Bracknell, D. C.

Jolliffe, I. and D. B. Stephenson, 2003: *Forecast verification. A practitioner's guide in atmospheric science.* 1 ed., Chichester, Wiley.

Jones, P., M. Hulme, and K. Briffa, 1993: A comparison of Lamb Circulation Types with an objective classification scheme. *International Journal of Climatology*, **13 (6)**, 655–663, doi:{10.1002/joc.3370130606}.

Kim, H.-M., P. J. Webster, and J. A. Curry, 2012: Seasonal prediction skill of ECMWF System 4 and

NCEP CFSv2 retrospective forecast for the Northern Hemisphere Winter. *Climate Dynamics*, **39 (12)**, 2957–2973, doi:{10.1007/s00382-012-1364-6}.

Klok, E. J. and A. M. G. K. Tank, 2009: Updated and extended European dataset of daily climate observations. *International Journal of Climatology*, **29 (8)**, 1182–1191, doi:{10.1002/joc.1779}.

Kristjansson, J. E., A. Staple, J. Kristiansen, and E. Kaas, 2002: A new look at possible connections between solar activity, clouds and climate. *Geophysical Research Letters*, **29 (23)**, doi:{10.1029/2002GL015646}.

Kutzbach, J., 1970: Large-scale features of monthly mean Northern Hemisphere anomaly maps of sea-level pressure. *Monthly Weather Review*, **98 (9)**, 708–&, doi:{10.1175/1520-0493(1970)098⟨0708:LSFOMM⟩2.3.CO;2}.

Labitzke, K., M. Kunzel, and S. Broennimann, 2006: Sunspots, the QBO and the stratosphere in the North Polar Region - 20 years later. *Meteorologische Zeitschrift*, **15 (3)**, 355–363, doi:{10.1127/0941-2948/2006/0136}, Colloquium in honor of Karin Labitzke on the Occasion of her 70th Birthday, Berlin, GERMANY, OCT 24, 2005.

Lamb, H., 1972: *British Isles weather types and a register of daily sequences of circulation patterns, 1861-1971*, Geophyiscal Memoir, Vol. 116. HMSO, London.

Lorenzo, M. N., J. J. Taboada, and L. Gimeno, 2008: Links between circulation weather types and teleconnection patterns and their influence on precipitation patterns in Galicia (NW Spain). *International Journal of Climatology*, **28 (11)**, 1493–1505, doi:{10.1002/joc.1646}.

Lorenzo, M. N., J. J. Taboada, I. Iglesias, and M. Gomez-Gesteira, 2011: Predictability of the spring rainfall in Northwestern Iberian Peninsula from sea surfaces temperature of ENSO areas. *Climatic Change*, **107 (3-4)**, 329–341, doi:{10.1007/s10584-010-9991-6}.

Michaelsen, J., 1987: Cross-validation in statitical climate forecast models. *Journal of Climate and Applied Meteorology*, **26 (11)**, 1589–1600, doi:{10.1175/1520-0450(1987)026⟨1589:CVISCF⟩2.0.CO;2}.

Mote, T. L. and E. R. Kutney, 2012: Regions of autumn Eurasian snow cover and associations with North American winter temperatures. *International Journal of Climatology*, **32 (8)**, 1164–1177, doi:{10.1002/joc.2341}.

Orsolini, Y., R. Senan, G. Balsamo, F. Doblas-Reyes, A. Vitart, A. Weisheimer, R. Carrasco, and R. Benestad, 2013: Impact of snow initialization on sub-seasonal forecasts. *Climate Dynamics*, doi:10.1007/s00382-013-1782-0.

Peings, Y., D. Saint-Martin, and H. Douville, 2012: A numerical sensitivity study of the influence of Siberian snow on the Northern Annular Mode. *Journal of Climate*, **25 (2)**, 592–607, doi:{10.1175/JCLI-D-11-00038.1}.

Polvani, L. M. and D. W. Waugh, 2004: Upward wave activity flux as a precursor to extreme stratospheric events and subsequent anomalous surface weather regimes. *Journal of Climate*, **17 (18)**, 3548–3554, doi:{10.1175/1520-0442(2004)017⟨3548:UWAFAA⟩2.0.CO;2}.

Ramsay, B. H., 1998: The interactive multisensor snow and ice mapping system. *Hydrological Processes*, **12 (10-11)**, 1537–1546, doi:{10.1002/(SICI)1099-1085(199808/09)12:10/11⟨1537::AID-HYP679⟩3.0.CO;2-A}.

Rodo, X., E. Baert, and F. Comin, 1997: Variations in seasonal rainfall in southern Europe during the present century: Relationships with the North Atlantic Oscillation and the El Nino Southern Oscillation. *Climate Dynamics*, **13 (4)**, 275–284, doi:{10.1007/s003820050165}.

Rodriguez-Fonseca, B. and M. de Castro, 2002: On the connection between winter anomalous precipitation in the Iberian Peninsula and North West Africa and the summer subtropical Atlantic sea surface temperature. *Geophysical Research Letters*, **29 (18)**, doi:{10.1029/2001GL014421}.

Rodriguez-Puebla, C., A. H. Encinas, and J. Saenz, 2001: Winter precipitation over the Iberian Peninsula and its relationship to circulation indices. *Hydrology and Earth System Science*, **5 (2, SI)**, 233–244.

Saito, K., J. Cohen, and D. Entekhabi, 2001: Evolution of atmospheric response to early-season Eurasian snow cover anomalies. *Monthly Weather Review*, **129 (11)**, 2746–2760, doi:{10.1175/1520-0493(2001)129⟨2746:EOARTE⟩2.0.CO;2}.

Smith, K. L., P. J. Kushner, and J. Cohen, 2011: The Role of Linear Interference in Northern Annular Mode Variability Associated with Eurasian Snow Cover Extent. *Journal of Climate*, **24 (23)**, 6185–6202, doi:{10.1175/JCLI-D-11-00055.1}.

Street, J., R. Carroll, and D. Ruppert, 1988: A note on computing robust regression estimates via iteratively reweighted least-squares. *American Statistican*, **42 (2)**, 152–154, doi:{10.2307/2684491}.

Tangang, F., W. Hsieh, and B. Tang, 1997: Forecasting the equatorial Pacific sea surface temperatures by neural network models. *Climate Dynamics*, **13 (2)**, 135–147, doi:{10.1007/s003820050156}.

Tank, A. M. G. K., et al., 2002: Daily dataset of 20th-century surface air temperature and precipitation series for the European Climate Assessment. *International Journal of Climatology*, **22 (12)**, 1441–1453, doi:{10.1002/joc.773}.

Taylor, K. E., R. J. Stouffer, and G. A. Meehl, 2012: An overview of CMIP5 and the experiment design. *Bull Am Meteor Soc*, **93 (4)**, 485–498, doi:{10.1175/BAMS-D-11-00094.1}.

Thompson, D. and J. Wallace, 1998: The Arctic Oscillation signature in the wintertime geopotential height and temperature fields. *Geophysical Research Letters*, **25 (9)**, 1297–1300, doi:{10.1029/98GL00950}.

Trenberth, K., 1984: Some effects of finite-sample size and persistence on meteorological statistics 1. Autocorrelations. *Monthly Weather Review*, **112 (12)**, 2359–2368, doi:{10.1175/1520-0493(1984)112⟨2359:SEOFSS⟩2.0.CO;2}.

Trigo, R. M. and C. C. DaCamara, 2000: Circulation weather types and their influence on the precipitation regime in Portugal. *International Journal of Climatology*, **20 (13)**, 1559–1581, doi:{10.1002/1097-0088(20001115)20:13⟨1559::AID-JOC555⟩3.0.CO;2-5}.

Vicente-Serrano, S. M., R. M. Trigo, J. I. Lopez-Moreno, M. L. R. Liberato, J. Lorenzo-Lacruz, S. Begueria, E. Moran-Tejeda, and A. El Kenawy, 2011: Extreme winter precipitation in the Iberian Peninsula in 2010: anomalies, driving mechanisms and future projections. *Climate Research*, **46 (1)**, 51–65, doi:{10.3354/cr00977}.

von Storch, H. and F. Zwiers, 1999: *Statistical Analysis in Climate Research*. Cambridge University Press, Cambridge.

Walker, G. and E. Bliss, 1932: World Weather V. *Memoirs of the Royal Meteorological Society*, **4 (36)**, 53–83.

Wilks, D., 2006: *Statistical methods in the atmospheric sciences*. 2 ed., Elsevier, Amsterdam.

Zappa, G., L. Shaffrey, and K. Hodges, 2013: The ability of CMIP5 models to simulate North Atlantic extratropical cyclones. *Journal of Climate*, doi:http://dx.doi.org/10.1175/JCLI-D-12-00501.1.

Zorita, E., V. Kharin, and H. von Storch, 1992: The atmospheric circulation and sea-surface temperature in the North Atlantic area in Winter - their interaction and relevance for Iberian precipitation. *Journal of Climate*, **5 (10)**, 1097–1108, doi:{10.1175/1520-0442(1992)005⟨1097:TACASS⟩2.0.CO;2}.

Table 1: Fraction (in %) of DJF-mean time series having a lag-1 autocorrelation coefficient ($r - lag1$) greater than $+0.25$. Row 1: name of the predictand variable and number of available time series / stations. Row 2: areal fraction for the original time series. Row 3: 90^{th} percentile of 2000 areal fractions obtained from randomly re-shuffling the DJF-mean values, i.e. critical value above which areal fractions in row 2 are globally significant ($\alpha_{global} = 0.10$, see text for more details). For each variable, the lowest areal fraction is printed in bold

Predictand Variable	$r - lag1 > +0.25$	**crit. value**
Precipitation amount (64)	**0**	22
Diurnal temperature range (66)	**5**	24
Sun hours (61)	**5**	26
Cloud cover (61)	**3**	28
Wind speed (62)	**19**	21

Table 2: Fraction of stations (in %) where the hindcast correlations obtained from cross-validation are locally significant ($\alpha_{local} = 0.05$). Column 1: Predictand/target variable. Columns 2-5: Fraction obtained from predicting with the October RSAI and SAI indices as well as with the October monthly-mean AO and NAO indices. For each variable, the highest areal fraction is printed in bold. Results are for DJF-mean values of the predictand variable.

Predictand Variable	**RSAI**	**SAI**	**AO**	**NAO**
Precipitation amount	**56**	52	0	2
Diurnal temperature range	**55**	52	8	0
Sun hours	**69**	53	7	2
Cloud cover	**72**	49	3	3
Wind speed	**36**	27	7	5

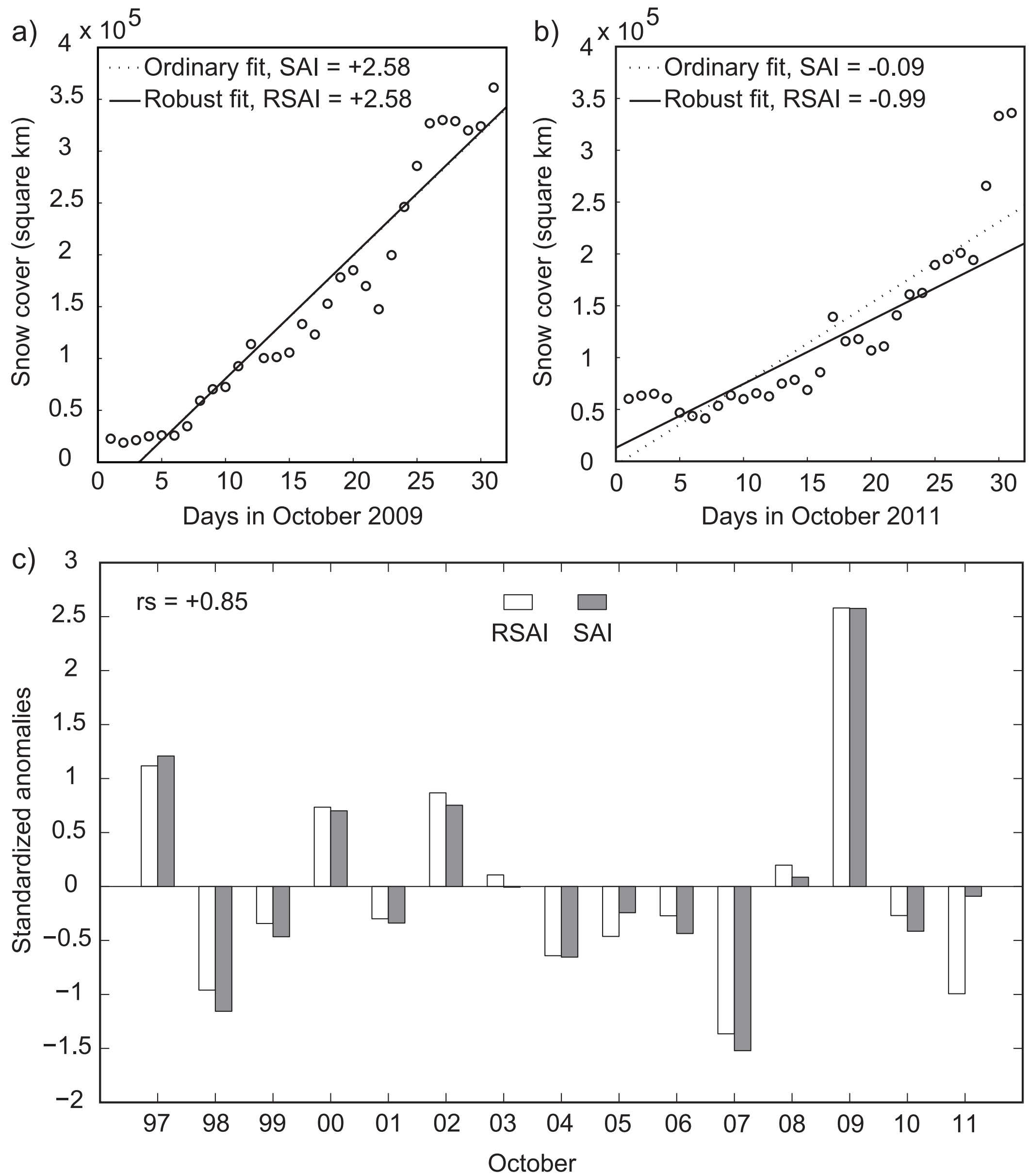

Figure 1: Eurasian snow cover for each day in (a) October 2009 and (b) October 2011 and the least squares fits obtained by ordinary vs. robust linear regression. The corresponding index values describing snow cover increase, defined as standardized anomalies of the respective regression coefficients are also displayed (SAI and RSAI). In October 2011, the differences between both index values are considerable due to outlier values at the end of the month. A comparison of the index time series and the corresponding Spearman correlation coefficient (rs) are shown in panel (c)

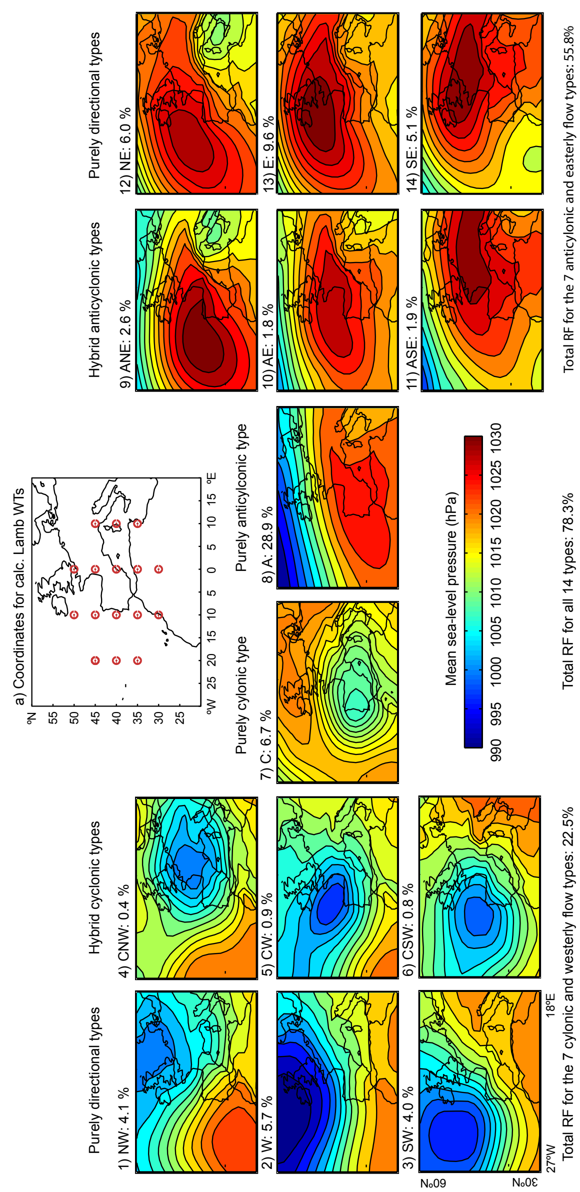

Figure 2: Composite maps for the circulation classes obtained from automated Lamb weather typing for the DJF days between 1997/98 to 2011/12, calculated upon instantaneous 12 UTC MSLP data from ERA-Interim. Only the 14 (out of 26) weather types relevant for the present study are displayed. On the left hand side, the cyclonic and westerly flow types are shown, on the right hand side, the anticyclonic and easterly flow types are shown. The panels are ordered to follow the cardinal directions and the total relative frequency of each WT is displayed above each panel. The coordinates used for computing the weather types are shown in panel (a).

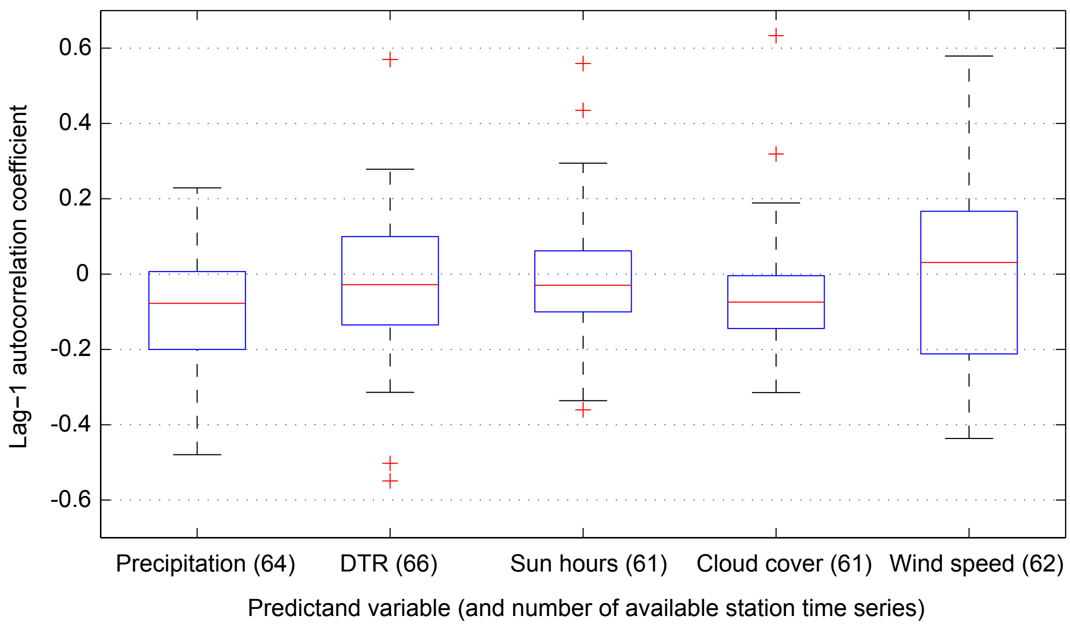

Figure 3: Distribution of the lag-1 autocorrelation coefficients of the applied time series, displayed by separate boxplots for each predictand variable. Bar: median, box: IQR, lower / upper limit of the whisker: 'last' data point not exceeding 1.5 times the IQR below / above the lower / upper quartile, cross: data point exceeding this threshold (i.e. outlier). For each predictand variable, the number of available station time series is displayed in parentheses

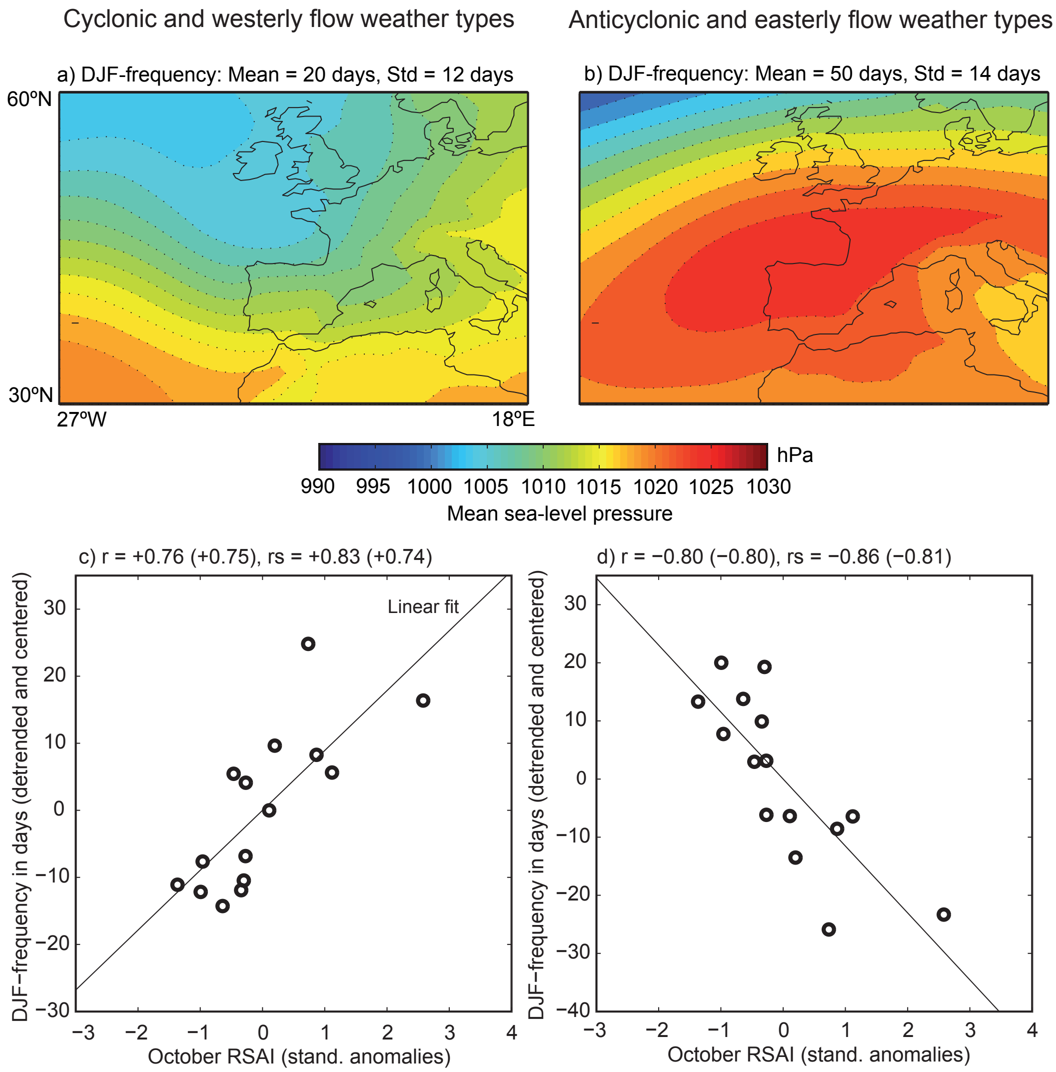

Figure 4: (a)+(b) Composite maps for the cyclonic and westerly flow weather types (see left hand side of Fig. 3) vs. anticyclonic and easterly flow weather types (see right hand side of Fig. 3); (c)+(d) Relationship between the Robust Snow Advance Index (RSAI) for October and the DJF-frequency of the above mentioned weather types (in days); the time series for these DJF-counts are detrended and centered to have zero-mean. Also shown are the Pearson (r) and Spearman (rs) correlation coefficients. Correlation coefficients for the original/non-detrended predictand time series are shown in parentheses.

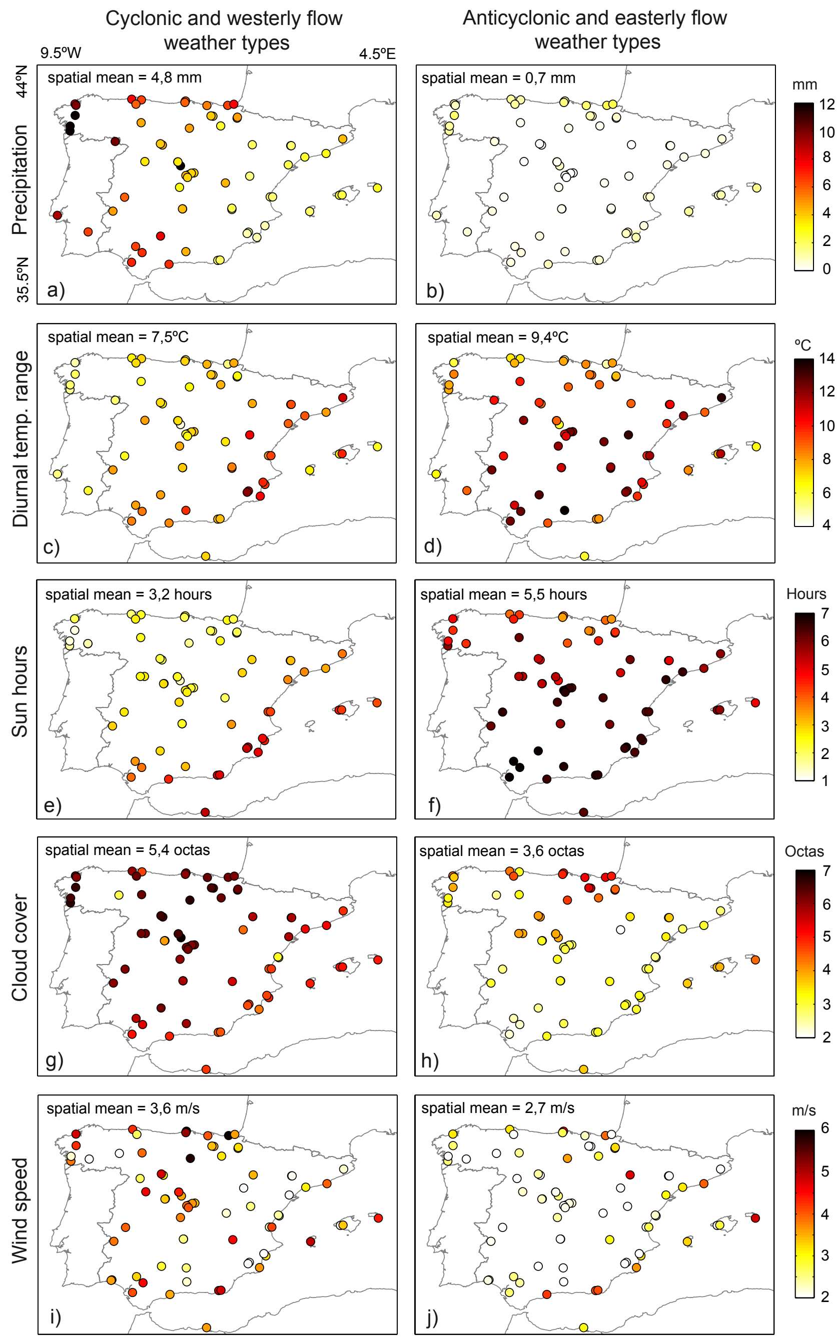

Figure 5: Left column: DJF-mean values conditioned on days corresponding to cyclonic and westerly flow weather types (left hand side of Fig. 3), Right column: DJF-mean values conditioned on days corresponding to anticyclonic and easterly weather types (right hand side of Fig. 3), for (a)+(b) precipitation amount, (c)+(d) diurnal temperature range, (e)+(f) sun hours, (g)+(h) cloud cover, (i)+(j) wind speed. The respective spatial mean values are displayed in the upper left corner of each panel.

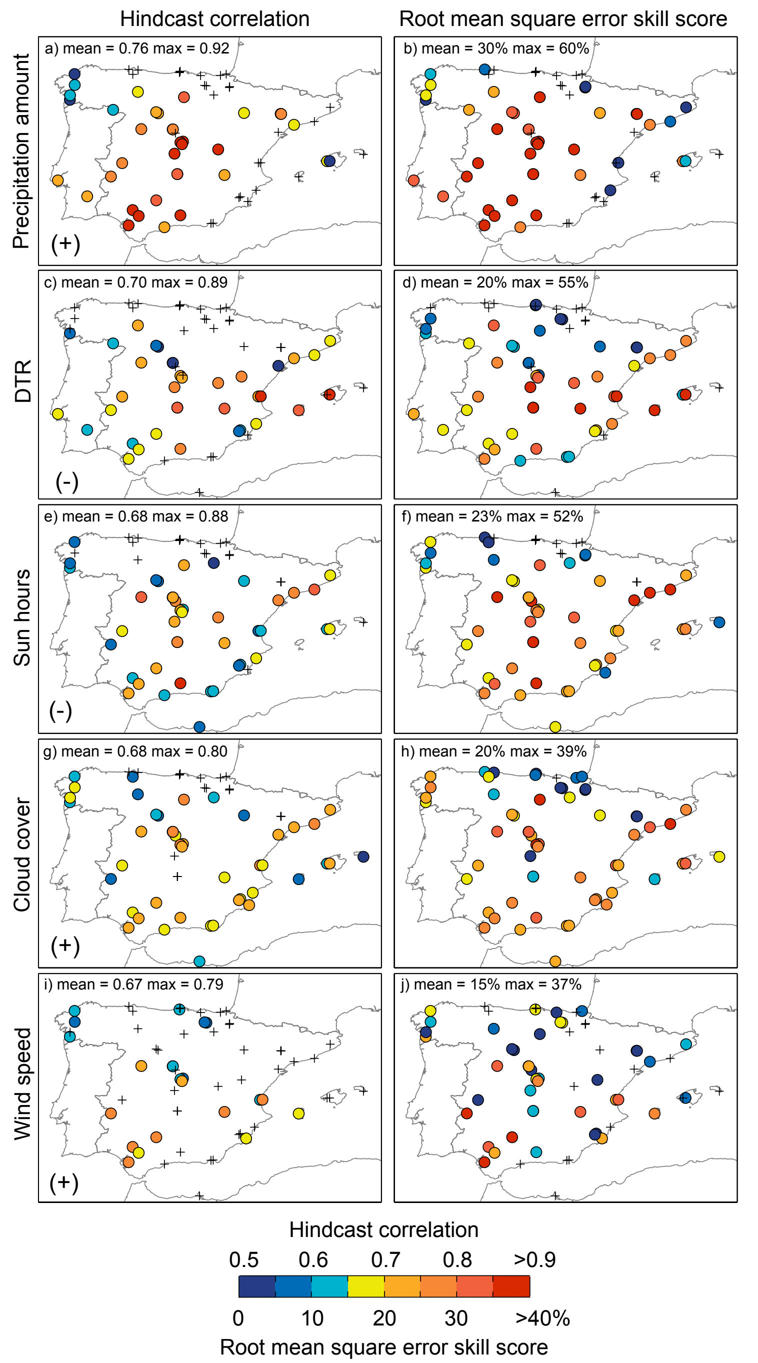

Figure 6: Hindcast skill obtained from cross-validation for: (a+b) precipitation amount, (c+d) diurnal temperature range (DTR), (e+f) sun hours, (g+h) cloud cover and (i+j) wind speed (DJF-mean values). Only significant ($\alpha_{local} = 0.05$) hindcast correlations (first column) and positive root mean square error skill scores (second column) are shown. The mean and maximum of the sig. hindcast correlations / positive skill scores and the sign of the Pearson correlation between the RSAI and the target variables are also given.